Optics Communications 390 (2017) 61–71

Contents lists available at ScienceDirect

Optics Communications

journal homepage: www.elsevier.com/locate/optcom

Subaperture stitching algorithms: A comparison

Shanyong Chen[a,b,*], Shuai Xue[a,b], Guilin Wang[a,b], Ye Tian[a,b]

[a] College of Mechatronic Engineering and Automation, National University of Defense Technology, 47 Yanzheng Street, Changsha, Hunan 410073, China
[b] Hunan Key Laboratory of Ultra-Precision Machining Technology, 47 Yanzheng Street, Changsha, Hunan, China

ARTICLE INFO

Keywords:
Subaperture stitching
Algorithm
Cylindrical surfaces
Surface metrology

ABSTRACT

With the research focus of subaperture stitching interferometry shifting from flat wavefronts to aspheric ones, a variety of algorithms for stitching optimization have been proposed. We try to category and compare the algorithms in this paper by their modeling of misalignment-induced subaperture aberrations which are of low orders. A simple way is to relate the aberrations to misalignment by linear approximation with small angle assumption. But it can not exactly model the induced aberrations of aspheres. In general, the induced aberrations can be fitted to free polynomials and then removed from subaperture measurements. However, it is at the risk of mixing up the surface error and the induced aberrations. The misalignment actually introduces different terms of aberrations with certain proportions. The interrelation is then determined through analytical modeling or ray tracing. The analytical model-based algorithm and the ray tracing-based algorithm both are tedious, aperture shape-related and surface type-specific. While the configuration space-based algorithm we proposed numerically calculates the surface height change under rigid body transformation, it is generally applicable to various surface types and different aperture shapes. Simulations and experiments are presented to compare the stitching results when different algorithms are applied to null cylindrical subapertures measured with a computer generated hologram. The configuration space-based algorithm shows superior flexibility and accuracy.

1. Introduction

Subaperture stitching interferometry enables test of large optics beyond the aperture and dynamic range of a standard interferometer because only a small subaperture of the optics is tested in a single measurement. Mechanical movement is required to align different subapertures to the test beam, which inevitably introduces misalignment and consequently results in change of optical path difference (OPD). It contributes to the subaperture wavefront aberrations and couples with the surface error. Stitching algorithms are then critical to bring all subaperture measurements together with misalignment-induced aberrations removed.

The change of single-pass OPD in the case of misalignment corresponds to the change of measured surface height in normal with respect to the reference surface. It can be divided into two components. The first one denoted by $\Delta\varphi_n$ is related to the nominal surface height change. It exists even if the test surface is ideal without any figure error. For example, a tilting plane changes its height coordinates related to the tilting angle. Hence in the simplest way, the change of OPD on the pixel (u,v) is linearly related to piston, tip and tilt as below:

$$\Delta\phi_n = a + bu + cv, \tag{1}$$

where a, b, and c are the coefficients of piston, tip and tilt. It works well for flat surfaces which are insensitive to lateral shift. Such a linear relationship is the result of first-order approximation of rigid body transformation under the small angle assumption, i.e., the tilting angle α is so small that $\sin\alpha$ can be approximated by α and $\cos\alpha$ by 1, respectively. However, Eq. (1) does not describe how the OPD changes with the change of lateral coordinates, e.g., in the case of lateral shift.

The second component of OPD change is related to the surface error itself, denoted by $\Delta\varphi_e$. It deals with the lateral coordinate change under misalignment such as lateral shift and clocking (rotation around Z axis). For the ideal surface without figure error, this component is nominally zero. The OPD change can be linearly related to the slope of surface height [1,2]:

$$\Delta\phi_e = p\frac{\partial\phi}{\partial u} + t\frac{\partial\phi}{\partial v} + \theta\left(u\frac{\partial\phi}{\partial v} - v\frac{\partial\phi}{\partial u}\right), \tag{2}$$

where p and t are the coefficients of lateral shift, θ is the clocking angle, and the partial derivatives are slopes in u and v directions, respectively. When testing aspheres with auxiliary null optics, Eq. (2) does not describe how the OPD changes with the change of null test condition. For an instance, the nominal asphere under test gives zero OPD in a

* Corresponding author at: College of Mechatronic Engineering and Automation, National University of Defense Technology, 47 Yanzheng Street, Changsha, Hunan 410073, China.
E-mail address: mesychen@163.com (S. Chen).

http://dx.doi.org/10.1016/j.optcom.2016.12.067
Received 11 November 2016; Received in revised form 19 December 2016; Accepted 27 December 2016

null test because the aspheric test wavefront modulated by the null optics exactly matches the measured surface. While the surface is misaligned, the test surface deviates from null test condition and significant aberrations such as coma and astigmatism arise in the measured wavefront. It can not be predicted by this slope-based model because the slope used here is not the slope of the aspheric surface sag in the Cartesian frame. It is the rate of variation of normal surface height with nominal surface sag subtracted.

A combination of Eqs. (1) and (2) seems a complete description of the OPD change induced by misalignments:

$$\Delta\phi = a + bu + cv + d(u^2 + v^2) + p\frac{\partial\phi}{\partial u} + t\frac{\partial\phi}{\partial v} + \theta\left(u\frac{\partial\phi}{\partial v} - v\frac{\partial\phi}{\partial u}\right), \quad (3)$$

where d is the coefficient of power (focus) and this term is included for testing spheres or aspheres. The OPD change is then optimally removed from the subaperture measurement based on the least-squares (LS) principle by minimizing the overlap mismatch as below:

$$F = \sum_{i=1}^{s-1}\sum_{k=i+1}^{s}\sum_{jo=1}^{{}^{ik}N_o}\left({}^{ik}\phi_{jo,i} + \Delta\phi_{jo,i} - {}^{ik}\phi_{jo,k} + \Delta\phi_{jo,k}\right)^2. \quad (4)$$

The left superscript "ik" indicates the overlap between subapertures i and k and ${}^{ik}N_o$ is the number of overlapping point pairs.

However, neither Eq. (1) nor Eq. (2) describes how aberrations are induced by misalignment of aspheric subapertures. When testing an asphere, optical metrologists are familiar with various aberrations induced by different misalignments. For an instance, tilt of an off-axis aspheric subaperture usually introduces astigmatism and coma to the wavefront aberration. It is not modeled in Eq. (3). With the research focus of subaperture stitching interferometry shifting from flat wavefronts to aspheric ones, a variety of algorithms for stitching optimization have been proposed [3–13]. The major difference lies in modeling of misalignment-induced subaperture aberrations. That is also the kernel of stitching optimization for aspheric subapertures. The algorithms are categorized into five groups in this paper. Comparative analysis is given and followed by simulation and experimental demonstration.

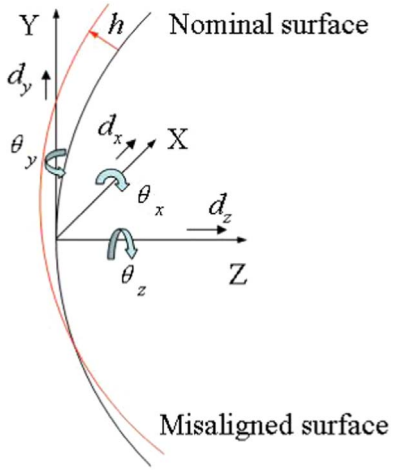

Fig. 1. Misaligned surface with six degrees of freedom.

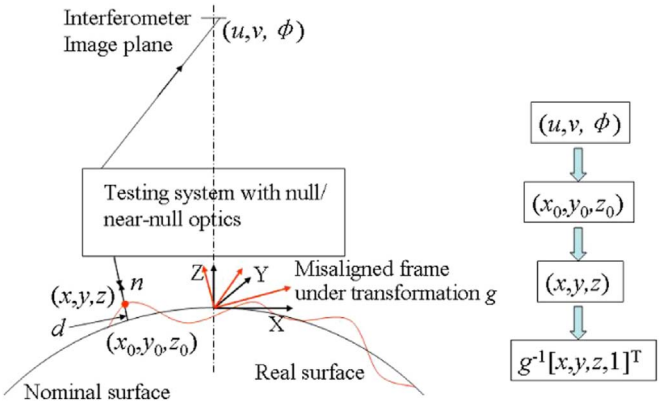

Fig. 2. Configuration space-based coordinate mapping.

2. Comparative analysis of subaperture stitching algorithms

2.1. Slope-based algorithm

Although there are a variety of subaperture stitching algorithms, they primarily boil down to solving the LS problem to minimize the overlap mismatch. Nevertheless, different way of modeling the misalignment-induced subaperture aberrations makes the algorithms different. The slope-based algorithm uses Eq. (3) to model the misalignment-induced aberrations. As mentioned above, it deals efficiently with lateral coordinate change which is related to the OPD change by the slope. It is advantageous when testing surface with significant middle to high-frequency error since the slope is quite big and OPD change is sensitive to the lateral coordinates change. A good example is stitching or registration of the continuous phase plates featured with vertical fluctuation of small amplitude and high frequency [14]. Pixel-scale lateral shift results in remarkable wavefront error and simple correction of piston, tip-tilt is insufficient.

The major disadvantage of the slope-based algorithm is its inefficiency of correcting the misalignment-induced aberrations for aspheres. Aberrations induced by misaligned aspheres are not only tip-tilt and power, but also more complex compound of secondary, tertiary and even higher orders.

2.2. Free polynomials correction

It is straightforward to describe the induced aberrations in polynomials and then best recognize the polynomial coefficients by minimizing the overlap mismatch. Generally Zernike polynomials are adopted which are orthogonal over a circular pupil and the low order terms are physically related to the Seidel aberrations such as the coma and astigmatism [15,16]. In such a way, the OPD change $\Delta\varphi$ includes the induced aberrations which are mostly coma and astigmatism:

$$\Delta\phi = c_0 + c_1u + c_2v + c_3(u^2 + v^2) + c_4(u^2 - v^2) + c_5uv + 3c_6u(u^2 + v^2) + 3c_7v(u^2 + v^2), \quad (5)$$

where c_0~c_7 are coefficients of piston, tip, tilt, power, astigmatism and coma, respectively. It can be considered as the augmented version of Eq. (1). And even more terms of Zernike polynomials can be included such as trefoil and high order coma and astigmatism. However, there are only six degrees of freedom for a rigid body motion, which means no more than six independent terms are allowed in the OPD change equation except the first three terms. As a result, if we include higher orders such as the trefoil, secondary coma and secondary astigmatism, their coefficients should not be independent. Otherwise it is at the risk of mixing up the surface error and the induced aberrations.

The misalignment actually introduces different terms of aberrations with certain proportions. The proportion of higher orders increases with both the numerical aperture (NA) of the test beam and the amount of higher order surface sag, which will be shown in the following subsections. Therefore it is possible to mistake the surface error for the induced aberrations if free polynomials are used. The interrelation between polynomial terms must be modeled exactly to describe the misalignment-induced aberrations.